Journal of Sound and Vibration (2002) **253**(4), 926–940
doi:10.1006/jsvi.2001.4058, available online at http://www.idealibrary.com on IDEAL®

ON THE STABILITY ANALYSIS OF SYSTEMS WITH INTERNAL RESONANCE

R. VEPA

*Department of Engineering, Queen Mary and Westfield College, Mile End Road, London E*1 4*NS, England. E-mail: r.vepa@uk.ac.qmw*

(*Received* 18 *December* 2000, *and in final form* 10 *July* 2001)

1. INTRODUCTION

The general problem considered is the stability analysis of systems exhibiting internal resonance such as those with a bifurcation point representing a Hopf bifurcation or a generalized Hopf bifurcation with non-semisimple double (or more) imaginary eigenvalues (case of 1 : 1 internal resonance). In the case of linear systems, the plant is characterized by multiple eigenvlaues on the imaginary axis and as rightly pointed out by Gajic and Lelic [1], by application of the Jordan canonical form, no definitive statement can be made about the stability of the system without further analysis. In fact, it is not really necessary to reduce it to the Jordan form to predict stability. In the case of non-linear systems, when there is the problem of internal resonances, it is well nigh impossible to calculate the individual modal transformations of modes that are in internal resonance with other modes. In such circumstances, all the modes that are in internal resonance must be dealt with jointly or it may be beneficial to avoid modal transformations altogether and reduce the equations to appropriate canonical forms and normal forms. The internal resonance case is important in a number of applications such as wind-induced oscillations of bundled conductors and aircraft longitudinal dynamics when the eigenvalues corresponding to a pair of elastic modes approach each other and the imaginary axis. Again, in the linear situation, the stability may be assessed by the application of Floquet theory and calculating the Floquet exponents. But the applications of Floquet exponents go beyond stability analysis. One approach to control system synthesis for a class of systems is based on the placement of the Floquet exponents or at least their magnitudes at appropriate locations in the $(-1, 1)$ domain. In fact, a popular approach to control law synthesis is to let the closed-loop exponents to be equal to zero. This controller, often referred to as the *dead beat controller*, then drives the response in the corresponding modes to their equilibrium points in a minimum number of time steps.

In these systems, a bifurcation-type analysis based on normal form reduction or other extended techniques based on Liapunov–Schmidt reduction or intrinsic harmonic balance can yield the dominant motion in the vicinity of the bifurcation point. It does not provide a solution which is uniformly valid over the entire phase space. Some of these systems are often characterized by a sequence of bifurcations leading to chaos and in addition to generating a local bifurcation diagram it is also essential to provide a complete response and ensure the local topological equivalence of solutions obtained by other methods. Direct numerical simulation is an invaluable tool in understanding some aspects of the response but is quite incapable of separating the woods from the trees. What is essential is

0022-460X/02/$35.00

a technique that would bridge the gap between local bifurcation analysis and direct numerical simulation.

The approach advocated in this paper shares some common ground with certain classical methods in vibrations such as the method of variation of parameters and the method of averaging. In the Krylov–Bogoliubov method of averaging, the governing equations for the amplitude dynamics are analytically averaged over a cycle to study the stability of vibration. In contrast to this method, the strategy adopted here is akin to a demodulation process whereby the amplitude dynamics is isolated but not averaged and then numerically integrated to evaluate the amplitude transition matrix over each step. Any apparent similarities to the Liapunov–Schmidt reduction of a typical bifurcation equation to a lower dimensional bifurcation equation is only incidental. However following a bifurcation-type analysis, the underlying behaviour of the vibration amplitude dynamics is first extracted. This is then employed in constructing a transformation of the equations so as to focus on the amplitude dynamics of the full non-linear (unabridged) system.

The objective of this study is to present a reasonably simple method of

(1) assessing the large amplitude stability of these systems;
(2) developing a numerical technique to predict the complete response of such systems as well as generate an amplitude parameter diagram and reveal features associated with instability and chaos.

An apparently abstract approach is adopted as the application spectrum includes stability analysis and postcritical bifurcation in non-linear structural dynamics, aeroelastic flutter, bifurcation in aircraft dynamics, helicopter dynamics and control and orbit and attitude control problems in space dynamics. The example selected, however, is an excellent benchmark problem and pertains to the phenomenon of galloping observed in conductor bundles and suspension cables in cable-stayed bridges. It can be identified, in the linear case, with the phenomenon of aeroelastic flutter characterized by the coalescence of two natural frequencies of the system. Thus, this results in an equal pair of imaginary eigenvalues which is also characteristic of the Hopf bifurcation and a 1 : 1 resonance.

There are indeed a number of analytical and numerical techniques, valid close to Hopf bifurcations or more complex mode interactions based on the methods of centre manifolds and normal forms. The bifurcations occurring as the linear stability is lost may be determined by the construction of a centre manifold. In particular, the nature of Hopf and more degenerate, higher codimensional bifurcations may be explicitly determined. There are also techniques for detecting Hopf bifurcations based on classical algebraic constructions to reduce the governing equations to normal form. They are known to be particularly well suited for solution by computer algebra techniques for vector fields of small or moderate dimension. Some of these methods also produce formulae on the asymptotic amplitude and stability of the limit cycle that are valid for any system of any arbitrary dimension (see for example references [2, 3] as well as a number of tutorials on the web). Unfortunately, they either rely on the existence of exact Jacobians for the construction of bialternate matrix products and on exact multivariate Taylor's series expansions. There are a number of examples in engineering when it is not possible to construct exact Jacobians or expand in a multivariate Taylor's series, i.e., either the region of convergence of the series is outside the domain of interest or the vector fields cannot be completely expressed in terms of analytic functions. It is such applications that are of primary interest in this paper. There are also a whole family of numerical continuation methods, which are very effective in determining the dependence of the solution, once it has been computed, on a particular parameter. In fact, continuation methods are particularly useful in determining limit cycles via the associated Floquet exponents. Such continuation

methods are in fact applicable to the Floquet exponents obtained in this paper but are not discussed here.

2. THEORETICAL BACKGROUND

The governing equations of motion about a bifurcation point, $\mathbf{x}(t) = 0$, are assumed to be non-linear of the form

$$\dot{\mathbf{x}}(t) = \mathbf{A}(\mathbf{x}; t, \mu)\mathbf{x}(t), \qquad \mathbf{x}(0) = \mathbf{x}_0, \tag{2.1}$$

where $\mathbf{A}(\mathbf{x}; t, \mu)$ is either independent of the time, t, or is periodic with period T, i.e., $\mathbf{A}(\mathbf{c}; t, \mu) = \mathbf{A}(c; t + T, \mu)$ when $\mathbf{x}(t) = \mathbf{c}$, a time-independent vector.

The matrix $\mathbf{A}(\mathbf{0}; t, \mu)$ determines the linearized motion about the bifurcation point, and is given by the state-transition matrix

$$\mathbf{x}_l(t) = \mathbf{\Phi}(t, 0; \mu)\mathbf{x}(0), \tag{2.2}$$

satisfying the linear equations

$$\dot{\mathbf{\Phi}}(t, 0; \mu) = \mathbf{A}(0; t, \mu)\mathbf{\Phi}(t, 0; \mu), \qquad \mathbf{\Phi}(0, 0; \mu) = \mathbf{I}. \tag{2.3}$$

The matrix $\mathbf{\Phi}(t, 0; \mu)$ is usually derived by numerical integration. Following the Floquet theory, $\mathbf{\Phi}(t, 0; \mu)$ can be expressed as

$$\mathbf{\Phi}(t, 0; \mu) = \mathbf{Z}(t)\exp(\mathbf{J}t)\mathbf{Z}^{-1}(0), \tag{2.4}$$

where, in general, $\exp(\mathbf{J}T)$ has diagonal real entries, as well as diagonal blocks of complex eigenvalues of the monodromy matrix $\mathbf{\Phi}(T, 0; \mu)$. When a pair of complex eigenvalues are equal it has the form

$$\exp(\mathbf{J}T) = \begin{bmatrix} \lambda_1 & \cdots & 0 & 0 & 0 & 0 & \cdots \\ \vdots & & \vdots & \vdots & \vdots & \vdots & \vdots \\ 0 & \cdots & \mathrm{Re}(\lambda_i) & \mathrm{Im}(\lambda_i) & 1 & 0 & \cdots \\ 0 & \cdots & -\mathrm{Im}(\lambda_i) & \mathrm{Re}(\lambda_i) & 0 & 1 & \cdots \\ 0 & \cdots & 0 & 0 & \mathrm{Re}(\lambda_i) & \mathrm{Im}(\lambda_i) & \cdots \\ 0 & \cdots & 0 & 0 & -\mathrm{Im}(\lambda_i) & \mathrm{Re}(\lambda_i) & \cdots \\ 0 & \cdots & 0 & 0 & 0 & 0 & \cdots \end{bmatrix} \tag{2.5}$$

and the matrix $\mathbf{Z}$ is the matrix of associated eigenvectors. From equation (2.4) it follows that $\dot{\mathbf{\Phi}}(T, 0; \mu)$ satisfies the equations

$$\begin{aligned} \dot{\mathbf{\Phi}}(t, 0; \mu) &= \dot{\mathbf{Z}}(t)\exp(\mathbf{J}t)\mathbf{Z}^{-1}(0) + \mathbf{Z}(t)\,\mathbf{J}\exp(\mathbf{J}t)\mathbf{Z}^{-1}(0) \\ &= (\dot{\mathbf{Z}}(t) + \mathbf{Z}(t)\mathbf{J})\exp(\mathbf{J}t)\mathbf{J}^{-1}(0) \end{aligned}$$

and since $\dot{\mathbf{\Phi}}(T, 0; \mu)$ also satisfies

$$\dot{\mathbf{\Phi}}(t, 0; \mu) = \mathbf{A}(0; t, \mu)\mathbf{\Phi}(t, 0; \mu) = \mathbf{A}(0; t, \mu)\mathbf{Z}(t)\exp(\mathbf{J}t)\mathbf{Z}^{-1}(0),$$

it follows that $\mathbf{Z}(t)$ satisfies the equation

$$\dot{\mathbf{Z}}(t) + \mathbf{Z}(t)\mathbf{J} = \mathbf{A}(0; t, \mu)\mathbf{Z}(t). \tag{2.6}$$

Moreover, by differentiating the identity, $\mathbf{Z}(t)\mathbf{Z}^{-1}(t) = \mathbf{I}$ one also has

$$\dot{\mathbf{Z}}^{-1}(t) = \mathbf{J}\mathbf{Z}^{-1}(t) - \mathbf{Z}^{-1}(t)\mathbf{A}(0; t, \mu). \tag{2.7}$$

At this stage the equations of motion are transformed, so as to focus on the governing amplitude dynamics. Although the use of a co-ordinate transformation based on the Jordan canonical form is a distinct possibility, the generation of the co-ordinate transformation is fraught with several computational difficulties. Thus, alternate approaches for constructing transformations of the response were explored. The transformation sought is a bounded time periodic function and is motivated by the interest being focused on the magnitude of the exponent of the motion rather than the exponent itself. In particular, it is necessary to isolate the dynamics of the amplitudes of periodic motion from the complete dynamics of the motion itself. Hence, as a first step, the following transformation based on the transition matrix is introduced as

$$\mathbf{x}(t) = \mathbf{\Phi}(t, 0; \mu)\mathbf{y}(t). \tag{2.8}$$

Differentiating equation (2.8), it follows that

$$\begin{aligned}\dot{\mathbf{x}}(t) &= \dot{\mathbf{\Phi}}(t, 0; \mu)\mathbf{y}(t) + \mathbf{\Phi}(t, 0; \mu)\dot{\mathbf{y}}(t)\\ &= \mathbf{A}(0; t, \mu)\mathbf{\Phi}(t, 0; \mu)\mathbf{y}(t) + \mathbf{\Phi}(t, 0; \mu)\dot{\mathbf{y}}(t).\end{aligned}$$

But from equations (2.1) and (2.8)

$$\dot{\mathbf{x}}(t) = \mathbf{A}(\mathbf{x}; t, \mu)\mathbf{x}(t) = \mathbf{A}(\mathbf{x}; t, \mu)\mathbf{\Phi}(t, 0; \mu)\mathbf{y}(t),$$

hence

$$\dot{\mathbf{y}}(t) = \mathbf{\Phi}^{-1}(t, 0; \mu)(\mathbf{A}(\mathbf{x}; t, \mu) - \mathbf{A}(0; t, \mu))\mathbf{\Phi}(t, 0; \mu)\mathbf{y}(t). \tag{2.9}$$

By letting,

$$\mathbf{F}(\mathbf{y}; t, \mu) = \mathbf{\Phi}^{-1}(t, 0; \mu)(\mathbf{A}(\mathbf{x}; t, \mu) - \mathbf{A}(0; t, \mu))\mathbf{\Phi}(t, 0; \mu) \tag{2.10}$$

it follows that

$$\dot{\mathbf{y}}(t) = \mathbf{F}(\mathbf{y}; t, \mu)\mathbf{y}(t), \quad \mathbf{y}(0) = \mathbf{x}_0, \tag{2.11}$$

where $\mathbf{F}(\mathbf{y}; t, \mu)$ is not necessarily periodic. However, one may eliminate the modes that are not in resonance by applying an appropriate modal transformation of the type discussed by Shaw and Pierre [4] although this is not an essential requirement. One thus assumes that the matrix $\exp(\mathbf{J}T)$ has no real eigenvalues and the complex eigenvalues are equal and in block Jordan form. Thus

$$\exp(\mathbf{J}T) = \begin{bmatrix} \mathrm{Re}(\lambda_i) & \mathrm{Im}(\lambda_i) & 1 & 0 \\ -\mathrm{Im}(\lambda_i) & \mathrm{Re}(\lambda_i) & 0 & 1 \\ 0 & 0 & \mathrm{Re}(\lambda_i) & \mathrm{Im}(\lambda_i) \\ 0 & 0 & -\mathrm{Im}(\lambda_i) & \mathrm{Re}(\lambda_i) \end{bmatrix}. \tag{2.12}$$

When the characteristic exponents of the transition matrix, $\mathbf{\Phi}(T, 0; \mu)$ lie on the unit circle, the matrix function $\mathbf{F}(\mathbf{y}; t, \mu)$ is periodic in t, i.e., $\mathbf{F}(\mathbf{a}; t, \mu) = \mathbf{F}(\mathbf{a}; t + T_i, \mu)$ for some fixed $\mathbf{a}$, a time-independent vector. Moreover, the stability of the system may be determined entirely from the properties of $\mathbf{F}(\mathbf{y}; t, \mu)$. It now follows that, $\mathbf{F}(\mathbf{a}; t, \mu)$ is periodic in t with period T_i for some fixed $\mathbf{a}$, whenever $\rho_i \to 1 - 0^+$, where $\lambda_i = \rho_i \exp(\mathrm{i}\theta_i)$. When $\rho_i = 1$, for some critical value of the parameter, $\mu = \mu_c$, the characteristic exponents of the associated Jordan form lie on the unit circle and yet $\mathbf{F}(\mathbf{a}; t, \mu)$ need not be periodic in t for some fixed $\mathbf{a}$. This is due to the presence of the so-called "*secular*" terms in the transition matrix, $\mathbf{\Phi}(T, 0; \mu)$, which are not really a problem for stability analysis unless the largest characteristic exponent associated with the solution $\mathbf{y}(t)$ is also exactly equal to unity. In these cases further analysis of the problem is essential.

Further, the matrix $\exp(\mathbf{J}T)$ is not in block Jordan form, but $\rho_i = \rho_j = 1$ and

$$\exp(\mathbf{J}T) = \begin{bmatrix} \mathrm{Re}(\lambda_i) & \mathrm{Im}(\lambda_i) & 0 & 0 \\ -\mathrm{Im}(\lambda_i) & \mathrm{Re}(\lambda_i) & 0 & 0 \\ 0 & 0 & \mathrm{Re}(\lambda_j) & \mathrm{Im}(\lambda_j) \\ 0 & 0 & -\mathrm{Im}(\lambda_j) & \mathrm{Re}(\lambda_j) \end{bmatrix}, \tag{2.13}$$

where either $\lambda_i \neq \lambda_j$ with $\lambda_i \approx \lambda_j$ or $\lambda_i = \lambda_j$ exactly, for some $\mu < \mu_c$, $\mathbf{F}(\mathbf{a}; t, \mu)$ is periodic in t with period T_i for some fixed $\mathbf{a}$ and again the stability of the system may be determined entirely from the properties of $\mathbf{F}(\mathbf{y}; t, \mu)$. Thus, in all the above cases the solution $\mathbf{y}(t)$ determines stability of the system.

Thus, the amplitude dynamics is governed by equations (2.10) and (2.11), and the vector $\mathbf{y}(t)$ may be referred to as the amplitude state vector. It is convenient to integrate these equations over a finite number (four or five in practice) of successive periods of the vibration using a Runge–Kutta–Fehlberg type of numerical integration method to construct an n cycle transition matrix. For convenience, in the rest of the paper the time period of vibration is assumed to remain constant and equal to $T = T_i$. It is important to distinguish between the amplitude state vector at a time instant, t_k, within a time period, $\mathbf{y}(t_k + nT)$ and the same vector at the end of the time period, $\mathbf{y}(T + nT)$. Local stability is governed by the transition from $\mathbf{y}(t_k + nT)$ to $\mathbf{y}(t_k + \Delta t_{k+1} + nT)$, while the stability of the solution over a period is governed by the transition from $\mathbf{y}(nT)$ to $\mathbf{y}(T + nT)$.

The solution, $\mathbf{y}(t_k + \Delta t_{k+1} + nT)$, during the $(n + 1)$th period and in the time interval $t_k < t < t_k + \Delta t_{k+1}$ may be determined by numerical integration and expressed in the form of a state transition solution as

$$\mathbf{y}(t_k + \Delta t_{k+1} + nT) = \Psi_{n+1}(\mathbf{y}(t_k + nT), t_k + \Delta t_{k+1} + nT, t_k + nT; \mu)\mathbf{y}(t_k + nT), \tag{2.14}$$

where $t_k = \sum_{j=0}^{k} \Delta t_j$.

As far as possible, the time steps, Δt_k, are all taken to be equal in practice although this is strictly not required. However, deciding on the best time step may require several iterations and is selected as the largest value for which Fehlberg error estimates are within acceptable bounds over the entire integration time frame.

Thus, the solution at the end of the kth time step may be written as

$$\mathbf{y}(t_k + nT) = \left[\prod_{j=0}^{k-1} \Psi_{n+1}(\mathbf{y}(t_j + nT), t_j \to \Delta t_{j+1} + nT, t_j + nT; \mu) \right] \mathbf{y}(nT). \tag{2.15}$$

Thus, the solution at the end of the $(n+1)$th period may be written as

$$\mathbf{y}(T+nT) = \left[\prod_{k=0}^{L-1} \Psi_{n+1}(\mathbf{y}(t_k+nT), t_k+\Delta t_{k+1}+nT, t_k+nT; \mu)\right]\mathbf{y}(nT), \tag{2.16}$$

where $t_L = T$.

The above equations may be expressed as

$$\mathbf{y}(t_k+nT) = \mathbf{\Phi}(t_k;\mu)\mathbf{y}(nT), \qquad \mathbf{y}(T+nT) = \mathbf{\Phi}(T;\mu)\mathbf{y}(nT) \tag{2.17, 2.18}$$

respectively.

3. COMPUTING THE STABILITY BOUNDARIES

Given a matrix eigenvalue problem in the form

$$(\mathbf{I}+\mathbf{A})\mathbf{x} = \lambda\mathbf{x}, \tag{3.1}$$

where $\mathbf{x}$ is an eigenvector of the matrix $\mathbf{A}$ and λ the corresponding eigenvalue, one may interpret the magnitude of the eigenvalue λ as the expansion or contraction rate of the eigenvector. Thus, the magnitude of the eigenvalue of the matrix

$$\mathbf{A}_{k+1} = \Psi_{n+1}(\mathbf{y}(t_k+nT_i), t_k+\Delta t_{k+1}+nT_i, t_k+nT_i;\mu) - \mathbf{I} \tag{3.2}$$

represents the local expansion/contraction rate of the corresponding eigenvector. Thus, one may define *aggregate local incremental expansion/contraction exponents* as the magnitudes of the eigenvalues of the weighted mean

$$\mathbf{A}_{mean} = \sum_{i=0}^{L-1} \frac{\Delta t_{nominal}}{\Delta t_{i+1}} \mathbf{A}_{i+1}\mathbf{Q}_{i+1}\mathbf{A}_{i+1}^{\mathrm{T}} \Big/ \sum_{i=0}^{L-1} \mathbf{Q}_{i+1}\mathbf{A}_{i+1}^{\mathrm{T}}. \tag{3.3}$$

In particular, if the weighting matrices $\mathbf{Q}_{i+1}$ are chosen such that

$$\mathbf{Q}_{i+1}^{-1} = \mathbf{A}_{i+1}^{\mathrm{T}}, \tag{3.4}$$

it follows that for this particular choice of $\mathbf{Q}_{i+1}$ the resulting expression for $\mathbf{A}_{mean}$ is

$$\begin{aligned}\mathbf{A}_{mean} &= \frac{1}{L}\sum_{j=0}^{L-1} \mathbf{A}_{j+1}\frac{\Delta t_{nominal}}{\Delta t_{j+1}} \\ &= \frac{1}{L}\sum_{j=0}^{L-1} (\Psi_{n+1}(\mathbf{y}(t_j+nT_i), t_j+\Delta t_{j+1}+nT_i, t_j+nT_i;\mu) - \mathbf{I})\frac{\Delta t_{nominal}}{\Delta t_{j+1}}.\end{aligned} \tag{3.5}$$

Thus, the *aggregate local expension/contraction exponents* over the entire time period, T_i, are given by the magnitudes of the eignevalues of the matrix

$$\mathbf{F} = (\mathbf{I}+\mathbf{A}_{mean})^{index}, \tag{3.6}$$

where $index = T_i/\Delta t_{nominal}$.

In the case of a linear system integrated by an exact method the two matrices $\mathbf{F}$ and $\mathbf{\Phi}(T_i;\mu)$ are identical, but this is not so in the non-linear case. Thus, one may define two sets of exponents as the magnitude of the eigenvalues of the two matrices $\mathbf{F}$ and $\mathbf{\Phi}(T_i;\mu)$ and

these are referred to as the *aggregate matrix* exponents and the *monodromy matrix* exponents. They are calculated in the next section for a typical example and compared with each other. Stability is guaranteed if the two sets of exponents are less than or utmost equal to unity.

It is worthwhile to note that if one were dealing with a linear time periodic problem, there would be no reason to distinguish between the exponents of the aggregate and monodromy matrices; they would be the same provided the integration time steps are assumed to be sufficiently small. In the non-linear case, there would be no reason to assume that they would be the same even when the integration time step is sufficiently small, as the system responses are basically amplitude dependent and the principle of superposition is not generally valid. Thus, there is the possibility of exploring both approaches for calculating the exponents.

Although equation (3.5) may be directly employed to evaluate the aggregate stability exponents, an alternate matrix is constructed to be consistent with the standard practice of evaluating the eigenvalues of the monodromy matrix in the case of linear time-varying systems.

4. ILLUSTRATIVE EXAMPLE

The example is the classic problem of wake-induced vibration of bundled overhead transmission lines exposed to strong crosswinds. A twin horizontal bundle of overhead transmission lines is considered. A mechanical model of this bundle consists of two rigid smooth cylinders, one of which is mounted on springs in the wake of the other identical but fixed neighbour. The two conductors lie in an almost horizontal plane, as shown in Figure 1, separated by a distance of about 10–25 conductor diameters and under certain conditions of wind velocity, the pair of conductors are dynamically unstable. These instabilities are due to the leeward conductor lying in the aerodynamically shed wake of the windward one. Apart from the conditions of instability, the post-critical behaviour in general and any limit cycles in the response are of interest. As in this example the motion of the conductors are known to diverge very slowly to a limit cycle oscillation, it is an eminently suitable benchmark problem for numerically assessing the postcritical behaviour of the class of systems exhibiting 1 : 1 internal resonance in the linear case.

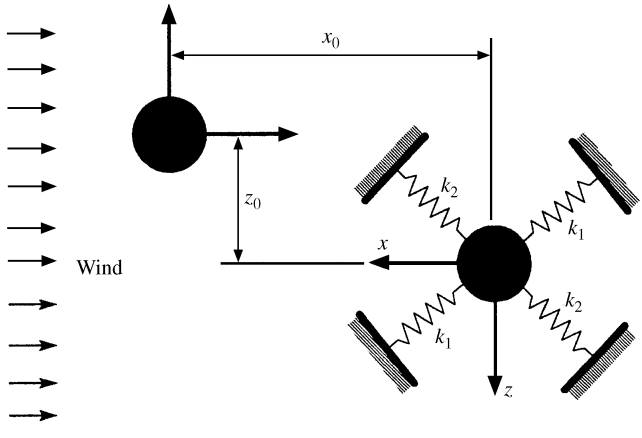

Figure 1. Illustration of an almost horizontal twin bundle of conductors.

The model of the twin conductor bundle assumes that the windward conductor is fixed while the leeward conductor is suspended by springs. The springs essentially represent a discretization of the elastic effects of the three-dimensional leeward conductor.

Referring to Simpson [5, 6], the governing equations of motion of the leeward conductor are given by

$$ml\ddot{\bar{x}} + (k_1 + k_2)\bar{x} + (k_1 - k_2)\bar{z} = F_x \qquad ml\ddot{\bar{z}} + (k_1 - k_2)\bar{x} + (k_1 + k_2)\bar{z} = F_x, \quad (4.1, 4.2)$$

where the springs are assumed to be symmetrically placed with respect to both the horizontal and vertical axes and the aerodynamic forces and

$$F_x = -\tfrac{1}{2}\rho l\bar{c}\,\bar{V}_r\{\bar{C}_D(\bar{V} + \dot{\bar{x}}) - \bar{C}_L\dot{\bar{z}}\}, \qquad F_z = -\tfrac{1}{2}\rho l\bar{c}\,\bar{V}_r\{\bar{C}_L(\bar{V} + \dot{\bar{x}}) + \bar{C}_D\dot{\bar{z}}\} \qquad (4.3)$$

with m being the mass of the conductor per unit length, l the conductor length, $\bar{c}$ the conductor diameter, $\rho = 1{\cdot}225\ \mathrm{kg/m^3}$, $\bar{x}, \bar{z}$ the horizontal and vertical displacements of the leeward conductor, $\bar{V}, \bar{V}_r$ the local and relative local wind speed, $b = \bar{V}/V$ the ratio of the local to the free stream velocity and $\bar{C}_L$ and $\bar{C}_D$ are the lift and drag coefficients based on the local wind speed. The $\bar{x}, \bar{z}$ displacements are non-dimensionalized and the result is

$$x = \bar{x}/\bar{c}, \qquad z = \bar{z}/\bar{c} \qquad (4.4)$$

and the horizontal and vertical spacing between the conductors is defined in non-dimensional co-ordinates.

The lift and drag models in equation (4.3) are based on standard representations of aerodynamic lift and drag in terms of empirically defined and experimentally determined coefficients commonly referred to as the coefficient of lift, $\bar{C}_L$ and the coefficient of drag, $\bar{C}_D$. The parameters $\bar{C}_L$ and $\bar{C}_D$ are functions of the state space in general and not constants. They are normally determined by experiment and are therefore only known at a finite number of discrete points in the state space. Based on potential flow models, it can be shown that the fundamental solutions for the velocity potential are exponentially dispersive in the downstream direction and essentially wave-like in the vicinity of the conductor bundle. On this basis a set of appropriate functions are use to model the coefficients of lift and drag rather than the polynomials used in reference [7]. While a detailed discussion of the accuracy of the modelling is not too relevant to the main thrust of the analysis, a qualitative justification for the approximate model may be provided based on the physics of potential flows. The physically meaningful modelling of these coefficients is strictly a matter of expediency as it permits the coefficients to be easily expanded in a Taylor's series without recourse to differentiation of numerical approximations to experimentally determined values. Further, as the original data quoted by Kern and Maitz [7] were not available, the approximation route was the only one open to the author.

The coefficients, $\bar{C}_D = \bar{C}_D(\hat{x}, \hat{z})$ and $\bar{C}_L = \bar{C}_L(\hat{x}, \hat{z})$ in equations (4.3) are then approximated, based on the plots of Kern and Maitz, as functions of $\hat{x} = x_0 - x$ and $\hat{z} = z_0 - z$, which are the relative distances of the leeward conductor from the windward conductor. Thus

$$b^2\bar{C}_D(\hat{x}, \hat{z}) = \tfrac{2}{3}\alpha(1 - \tfrac{1}{2}\cos(\hat{z})\exp(-(|\hat{x}| - 5)/50)), \quad \alpha = 1{\cdot}2, \quad -\pi \leqslant z \leqslant \pi,$$

$$= \tfrac{2}{3}\alpha(1 + \tfrac{1}{2}\exp(-(|x| - 5)/50), \quad \pi > z > \pi, \qquad (4.5)$$

$$b^2\bar{C}_L(\hat{x}, \hat{z}) = -(\alpha/4)\sin(\hat{z})\exp(-(|x| - 5)/15) = 0, \quad -\pi \leqslant z \leqslant \pi. \qquad (4.6)$$

When $\hat{x}$ is less than zero, the roles of the leeward and windward conductors are reversed. However, since only relative motion is considered and the windward conductor is assumed fixed, forces acting on the windward conductor are assumed to be acting on the leeward conductor with their directions reversed. Effectively, this means that $\bar{C}_D(\hat{x}, \hat{z})$ reverses sign when $\hat{x}$ is less than zero.

For sufficiently small and positive values of $\hat{x}$ and $\hat{z}$, the derivatives of the above expressions are

$$\begin{aligned}
b^2\,\partial\bar{C}_D/\partial x &= -\tfrac{2}{300}\,\alpha\cos(\hat{z})\exp(-(\hat{x}-5)/50),\\
b^2\,\partial\bar{C}_L/\partial x &= -(\alpha/60)\sin(\hat{z})\exp(-(\hat{x}-5)/15),\\
b^2\,\partial\bar{C}_D/\partial z &= -\tfrac{1}{3}\,\alpha\sin(\hat{z})\exp(-(\hat{x}-5)/50),\\
b^2\,\partial\bar{C}_L/\partial z &= (\alpha/4)\cos(\hat{z})\exp(-(\hat{x}-5)/15).
\end{aligned} \tag{4.7}$$

Further,

$$\bar{V}_r = \sqrt{(\bar{V}+\dot{\hat{x}})^2 + \dot{\hat{z}}^2} \tag{4.8}$$

and the equations of motion may be expressed as

$$\begin{aligned}
&\ddot{x} + (1/ml)(k_1+k_2)x + (1/ml)(k_1-k_2)z\\
&\quad = -\tfrac{1}{2}(\rho V^2 b^2/m)\sqrt{(1+\bar{c}\dot{x}/bV)^2 + (\bar{c}\dot{z}/bV)^2}\,\{\bar{C}_D(1+\bar{c}\dot{x}/bV) - \bar{C}_L\bar{c}\dot{z}/bV\},
\end{aligned} \tag{4.9}$$

$$\begin{aligned}
&\ddot{z} + (1/ml)(k_1-k_2)x + (1/ml)(k_1+k_2)z\\
&\quad = -\tfrac{1}{2}(\rho V^2 b^2/m)\sqrt{(1+\bar{c}\dot{x}/bV)^2 + (\bar{c}\dot{z}/bV)^2}\,\{\bar{C}_L(1+\bar{c}\dot{x}/bV) + \bar{C}_D\bar{c}\dot{z}/bV\}.
\end{aligned} \tag{4.10}$$

Given that $\omega_1^2 = 2k_1/ml$ and $\omega_2^2 = 2k_2/ml$, the above equations of motion may be expressed as

$$\begin{aligned}
&\ddot{x} + ((\omega_1^2+\omega_2^2)/2)x + ((\omega_1^2-\omega_2^2)/2)z\\
&\quad = -\tfrac{1}{2}(pV^2 b^2/m)\sqrt{(1+\bar{c}\dot{x}/bV)^2 + (\bar{c}\dot{z}/bV)^2}\,\{\bar{C}_D(1+\bar{c}\dot{x}/bV) - \bar{C}_L\bar{c}\dot{z}/bV\},
\end{aligned} \tag{4.11}$$

$$\begin{aligned}
&\ddot{z} + ((\omega_1^2-\omega_2^2)/2)x + ((\omega_1^2+\omega_2^2)/2)z\\
&\quad = -\tfrac{1}{2}(pV^2 b^2/m)\sqrt{(1+\bar{c}\dot{x}/bV)^2 + (\bar{c}\dot{z}/bV)^2}\,\{\bar{C}_L(1+\bar{c}\dot{x}/bV) + \bar{C}_D\bar{c}\dot{z}/bV\}.
\end{aligned} \tag{4.12}$$

Expanding the equations in a Taylor's series and retaining terms up to first order results in

$$\begin{aligned}
&\ddot{x} + ((\omega_1^2+\omega_2^2)/2)x + ((\omega_1^2-\omega_2^2)/2)z\\
&= -\tfrac{1}{2}(\rho V^2 b^2/m)\{\bar{C}_D(1+2\bar{c}\dot{x}/bV) - \bar{C}_L\bar{c}\dot{z}/bV + (\partial\bar{C}_D/\partial x)(x-x_e) + (\partial\bar{C}_D/\partial z)(z-z_e)\},
\end{aligned} \tag{4.13}$$

$$\begin{aligned}
&\ddot{z} + ((\omega_1^2-\omega_2^2)/2)x + ((\omega_1^2+\omega_2^2)/2)z\\
&= -\tfrac{1}{2}(\rho V^2 b^2/m)\{\bar{C}_L(1+2\bar{c}\dot{x}/bV) + \bar{C}_D\bar{c}\dot{z}/bV + (\partial\bar{C}_L/\partial x)(x-x_e) + (\partial\bar{C}_L/\partial z)(z-z_e)\},
\end{aligned} \tag{4.14}$$

where the coefficients, $\bar{C}_D = \bar{C}_D(\hat{x}_e, \hat{z}_e)$ and $\bar{C}_L = \bar{C}_L(\hat{x}_e, \hat{z}_e)$ are evaluated at the equilibrium position, (x_e, z_e), where $\hat{x}_e = x_0 - x_e$ and $\hat{z}_e = z_0 - z_e$.

By letting $u = x + z$ and $v = x - z$,

$$\ddot{u} + \omega_1^2 u = -\frac{1}{2}\frac{\rho V^2 b^2}{m}\left\{(\bar{C}_D + \bar{C}_L)\left(1 + \frac{\bar{c}(\dot{u} + \dot{v})}{bV}\right) + (\bar{C}_D - \bar{C}_L)\frac{\bar{c}(\dot{u} - \dot{v})}{2bV} + f_1\right\}, \quad (4.15)$$

$$\ddot{v} + \omega_2^2 v = -\frac{1}{2}\frac{\rho V^2 b^2}{m}\left\{(\bar{C}_D - \bar{C}_L)\left(1 + \frac{\bar{c}(\dot{u} + \dot{v})}{bV}\right) - (\bar{C}_D + \bar{C}_L)\frac{\bar{c}(\dot{u} - \dot{v})}{2bV} + f_2\right\}, \quad (4.16)$$

where

$$\begin{bmatrix} f_1 \\ f_2 \end{bmatrix} = -\frac{1}{2}\frac{\rho V^2 b^2}{m}\begin{bmatrix} \left(\frac{\partial \bar{C}_D}{\partial x} + \frac{\partial \bar{C}_D}{\partial z} + \frac{\partial \bar{C}_L}{\partial x} + \frac{\partial \bar{C}_L}{\partial z}\right)(u - u_e) + \left(\frac{\partial \bar{C}_D}{\partial x} - \frac{\partial \bar{C}_D}{\partial z} + \frac{\partial \bar{C}_L}{\partial x} - \frac{\partial \bar{C}_L}{\partial z}\right)(v - v_e) \\ \left(\frac{\partial \bar{C}_D}{\partial x} + \frac{\partial \bar{C}_D}{\partial z} - \frac{\partial \bar{C}_L}{\partial x} - \frac{\partial \bar{C}_L}{\partial z}\right)(u - u_e) + \left(\frac{\partial \bar{C}_D}{\partial x} - \frac{\partial \bar{C}_D}{\partial z} - \frac{\partial \bar{C}_L}{\partial x} + \frac{\partial \bar{C}_L}{\partial z}\right)(v - v_e) \end{bmatrix}$$
$$= -\mathbf{K}_{aero}\begin{bmatrix} u - u_e \\ v - v_e \end{bmatrix} \quad (4.17)$$

and the derivatives are evaluated at the equilibrium points.

Under steady state conditions at the equilibrium point

$$\omega_1^2 u_e = -\tfrac{1}{2}(\rho V^2 b^2/m)(\bar{C}_D + \bar{C}_L), \qquad \omega_2^2 v_e = -\tfrac{1}{2}(\rho V^2 b^2/m)(\bar{C}_D - \bar{C}_L). \quad (4.18)$$

Hence, the equations for u and v may be written as

$$\ddot{u} + \omega_1^2(u - u_e) = -\frac{1}{2}\frac{\rho V^2 b^2}{m}\left\{(3\bar{C}_D + \bar{C}_L)\frac{\bar{c}\dot{u}}{2bV} + (\bar{C}_D + 3\bar{C}_L)\frac{\bar{c}\dot{v}}{4bV}\right\} - k_{aero,11}(u - u_e) - k_{aero,12}(v - v_e), \quad (4.19)$$

$$\ddot{v} + \omega_2^2(v - v_e) = -\frac{1}{2}\frac{\rho V^2 b^2}{m}\left\{(\bar{C}_D - 3\bar{C}_L)\frac{\bar{c}\dot{u}}{2bV} + (3\bar{C}_D - \bar{C}_L)\frac{\bar{c}\dot{v}}{4bV}\right\} - k_{aero,21}(u - u_e) - k_{aero,22}(v - v_e) \quad (4.20)$$

and the characteristic equation for the system takes the form

$$\lambda^4 + a_1\lambda^3 + a_2\lambda^2 + a_3\lambda + a_4 = 0, \quad (4.21)$$

where

$$a_1 = (c_{22} + c_{11}), \qquad a_2 = (\omega_2^2 + \omega_1^2 + k_{aero,22} + k_{aero,11} + |c_{ij}|),$$

$$a_3 = (c_{11}\omega_2^2 + c_{22}\omega_1^2 + c_{11}k_{aero,22} + c_{22}k_{aero,11} - c_{12}k_{aero,21} - c_{21}k_{aero,12}),$$

$$a_4 = \omega_1^2\omega_2^2 + k_{aero,11}\omega_2^2 + k_{aero,22}\omega_1^2 + k_{aero,11}k_{aero,22} - k_{aero,12}k_{aero,21}$$

and the coefficients c_{ij} are the elements of the matrix $\mathbf{C}$ defined by

$$\mathbf{C} = \begin{bmatrix} c_{11} & c_{12} \\ c_{21} & c_{22} \end{bmatrix} = \frac{1}{8}\frac{\rho \bar{c} V b}{m} \begin{bmatrix} 6\bar{C}_D + 2\bar{C}_L & \bar{C}_D + 3\bar{C}_L \\ 2\bar{C}_D - 6\bar{C}_L & 3\bar{C}_D - \bar{C}_L \end{bmatrix} = \sigma \begin{bmatrix} 6\bar{C}_D + 2\bar{C}_L & \bar{C}_D + 3\bar{C}_L \\ 2\bar{C}_D - 6\bar{C}_L & 3\bar{C}_D - \bar{C}_L \end{bmatrix}.$$

Applying the Routh–Hurwitz criterion leads to the criterion for the stability of the equilibrium solution and is

$$a_i > 0, \quad i = 1, 2, 3, 4, \qquad a_1 a_2 a_3 > a_3^2 + a_1^2 a_4. \tag{4.22}$$

The approach in the following is somewhat similar to the strategy adopted in Hopf bifurcation analysis where damping is initially neglected to isolate the underlying behaviour in the vicinity of a bifurcation point. In practice, however, damping is not neglected in solving the full non-linear problem.

Thus, if one assumes that a_1 and a_3 are both negligible and hence equal to zero, the condition for a 1 : 1 resonance is

$$\omega_2^2 + \omega_1^2 + k_{aero,22} + k_{aero,11} + |c_{ij}| = 2\sqrt{\omega_1^2\omega_2^2 + k_{aero,11}\omega_2^2 + k_{aero,22}\omega_1^2 + k_{aero,11}k_{aero,22}\omega_2^2 - k_{aero,12}k_{aero,21}}, \tag{4.23}$$

where $|c_{ij}| = \sigma^2 \times 16 \times (C_D^2 + C_L^2)$. The condition may be expressed as

$$(\omega_1 - \omega_2) + |c_{ij}| = -k_{aero,22} - k_{aero,11} + 2\sqrt{\omega_1^2\omega_2^2 + k_{aero,11}\omega_2^2 + k_{aero,22}\omega_1^2 + k_{aero,11}k_{aero,22} - k_{aero,12}k_{aero,21}} - 2\omega_1\omega_2. \tag{4.24}$$

As this stage, it is initially assumed that the contribution of the damping terms, i.e., $|c_{ij}|$ is negligible. This permits one to generate the time periodic transformation which is then used to exact the amplitude dynamics from the full non-linear equations of motion without ignoring the contribution of aerodynamic or any other damping.

Ignoring $|c_{ij}|$, the equation reduces to

$$(\omega_1 - \omega_2)^2 + 2\omega_1\omega_2 = \omega_1^2 + \omega_2^2 = -k_{aero,22} - k_{aero,11} + 2\sqrt{\omega_1^2\omega_2^2 + k_{aero,11}\omega_2^2 + k_{aero,22}\omega_1^2 + k_{aero,11}k_{aero,22} - k_{aero,12}k_{aero,21}} \tag{4.25}$$

After estimating an initial starting value of the critical velocity, the corresponding equilibrium solutions are then determined by minimizing the absolute value of the error,

$$e = \omega_2^2 + \omega_1^2 + k_{aero,22} + k_{aero,11} - 2\sqrt{\omega_1^2\omega_2^2 + k_{aero,11}\omega_2^2 + k_{aero,22}\omega_1^2 + k_{aero,11}k_{aero,22} - k_{aero,12}k_{aero,21}}. \tag{4.26}$$

At the critical velocity the linear undamped equations may be reduced to the standard Jordon canonical form exhibiting a 1 : 1 internal resonance.

4.1. MOTION ABOUT THE EQUILIBRIUM POINT UNDER CRITICAL CONDITIONS

Consider first the linearized motion about the equilibrium point under critical conditions. The governing linear equations assuming all damping is negligible are

$$\ddot{x} + \left(\frac{\omega_1^2 + \omega_2^2}{2} + \frac{1}{2}\frac{\rho V_{crit}^2 b^2}{m}\frac{\partial \bar{C}_D}{\partial x}\right)(x - x_e) + \left(\frac{\omega_1^2 - \omega_2^2}{2} + \frac{1}{2}\frac{\rho V_{crit}^2 b^2}{m}\frac{\partial \bar{C}_D}{\partial z}\right)(z - z_e) = 0,$$

$$\ddot{z} + \left(\frac{\omega_1^2 - \omega_2^2}{2} + \frac{1}{2}\frac{\rho V_{crit}^2 b^2}{m}\frac{\partial \bar{C}_L}{\partial x}\right)(x - x_e) + \left(\frac{\omega_1^2 + \omega_2^2}{2} + \frac{1}{2}\frac{\rho V_{crit}^2 b^2}{m}\frac{\partial \bar{C}_L}{\partial z}\right)(z - z_e) = 0, \tag{4.27}$$

where the derivatives are evaluated at the equilibrium position. The linearized equations of motion govern the small amplitude motions relative to the spacing between the conductors when the circulatory aerodynamic stiffness effects are predominantly greater than the aerodynamic damping effects. Under the circumstances of a high freestream velocity relative to the velocities of the conductor the aerodynamic damping effects may be ignored.

The complete non-linear equations are

$$\ddot{x} + ((\omega_1^2 + \omega_2^2)/2)(x - x_e) + ((\omega_1^2 - \omega_2^2)/2)(z - z_e)$$

$$= -\frac{1}{2}\frac{\rho V_{crit}^2 b^2}{m}\left\{\sqrt{\left(1 + \frac{\bar{c}\dot{x}}{bV_{crit}}\right)^2 + \left(\frac{\bar{c}\dot{z}}{bV_{crit}}\right)^2}\left\{\bar{C}_D\left(1 + \frac{\bar{c}\dot{x}}{bV_{crit}}\right) - \bar{C}_L\frac{\bar{c}\dot{z}}{bV_{crit}}\right\} - \bar{C}_D(\hat{x}_e, \hat{z}_e)\right\}$$

and

$$\ddot{z} + ((\omega_1^2 - \omega_2^2)/2)(x - x_e) + ((\omega_1^2 + \omega_2^2)/2)(z - z_e)$$

$$= -\frac{1}{2}\frac{\rho V_{crit}^2 b^2}{m}\left\{\sqrt{\left(1 + \frac{\bar{c}\dot{x}}{bV_{crit}}\right)^2 + \left(\frac{\bar{c}\dot{z}}{bV_{crit}}\right)^2}\left\{\bar{C}_L\left(1 + \frac{\bar{c}\dot{x}}{bV_{crit}}\right) + \bar{C}_D\frac{\bar{c}\dot{z}}{bV_{crit}}\right\} - \bar{C}_L(\hat{x}_e, \hat{z}_e)\right\}, \tag{4.28}$$

where the coefficients, $\bar{C}_D = \bar{C}_D(\hat{x}, \hat{z})$ and $\bar{C}_L = \bar{C}_L(\hat{x}, \hat{z})$ are evaluated in terms of $\hat{x} = x_0 - x$ and $\hat{z} = z_0 - z$. One may then express the two sets of equations in terms of the state vector

$$\mathbf{x} = [x - x_e \;\; \dot{x} \;\; z - z_e \;\; \dot{z}]^{\mathrm{T}}$$

integrate the state equations, and compute the stability boundaries by the methods presented above.

4.2. NUMERICAL EXAMPLE

The numerical example considered was similar to the one considered by Kern and Maitz [7]. However, not only a different value had to be selected for velocity ratio, b, the aerodynamic lift and drag coefficients data presented graphically by Kern and Maitz were approximated using different basis functions. It was felt that these basis functions were more appropriate from the standpoint of the physics problem. However, the qualitative results obtained for the undamped linear case were not different from those of Kern and Maitz.

One of the problems faced was defining the so-called critical velocity when both the eigenvalues are equal. Unfortunately, this can never be exactly obtained and lower and

TABLE 1

Parameter values for numerical example

Parameter	Value	Parameter	Value
c (conductor dia.)	0·03048 m	Critical frequency	7·997 rad/s
ω_2 (Highest nat. freq.)	8·34 rads/s	b (reference value)	1·0
ω_1/ω_2 (ratio of natural frequencies)	0·91	x_0 (leeward conductor x-position reference to windward conductor)	12 (in units of conductor diameter)
ρ (air density)	1·225 kg/m^3	z_0 (leeward conductor z-position reference to windward conductor)	− 1·4
m (mass per unit length)	1·596 kg/m	x_e (leeward conductor equilibrium x-displacement	− 0·2081
Critical wind velocity (v_c)	6·8226 m/s	z_e (leeward conductor equilibrium z-displacement)	− 0·07019
Wind velocity used for computing the response	$v_c^- \approx v_c$ − 1·0E − 17 m/s	Number of integration time steps	300/cycle

upper bounds must be estimated in practice. The issue here is not the precision of the computation but to ensure that one is sufficiently close to the 1 : 1 internal resonance case. The values of the critical velocity bounds and the critical frequency are listed in Table 1. However, it must be emphasized that only bounds can be calculated to this velocity and that one can get arbitrarily close to the condition of 1 : 1 resonance but *never* really obtain exactly equal eigenvalues. This is not really a problem in this methodology as no attempt is made to reduce the linear equations to a Jordan canonical form. In this example, only the lower bound was utilized in the computation of the stability exponents and was computed as close to the critical velocity as was possible (within 1·0E-17 of the critical velocity).

The numerical integration was performed using Runge–Kutta–Fehlberg method as this provided an estimate of the error during each step. A two-pass approach was adopted to ensure that the error estimate was acceptable and below a specified tolerance value over the entire integration time frame. In this manner, the maximum acceptable integration stepsize was chosen. A typical plot illustrating the motion of the leeward conductor is shown in Figure 2. For lower amplitudes, the motion slowly diverged to a limit cycle while for higher amplitudes the motion slowly converged onto it.

The magnitude of the maximum and minimum exponents computed over a *four-cycle* period by both the methods mentioned above was then plotted against a representative amplitude parameter. The single-cycle exponents may be obtained from these by taking the fourth root of each of the exponents. These plots are illustrated in Figure 3 clearly indicating the existence of a limit cycle for an amplitude parameter ≈ 62. At this value of the amplitude parameter, the minimum and maximum exponents are equal to each other and also equal to unity. The minimum exponents obtained by the two methods are almost identical. This is not entirely unexpected as the minimum exponent below the limit cycle is usually unity, while the minimum exponent above the limit cycle is less than unity. Minimum exponents correspond to stable components of the motion. As the exponents of unstable motion are generally difficult to estimate, the maximum discrepancy would be expected in the maximum exponents corresponding to the unstable domain which is below the limit cycle.

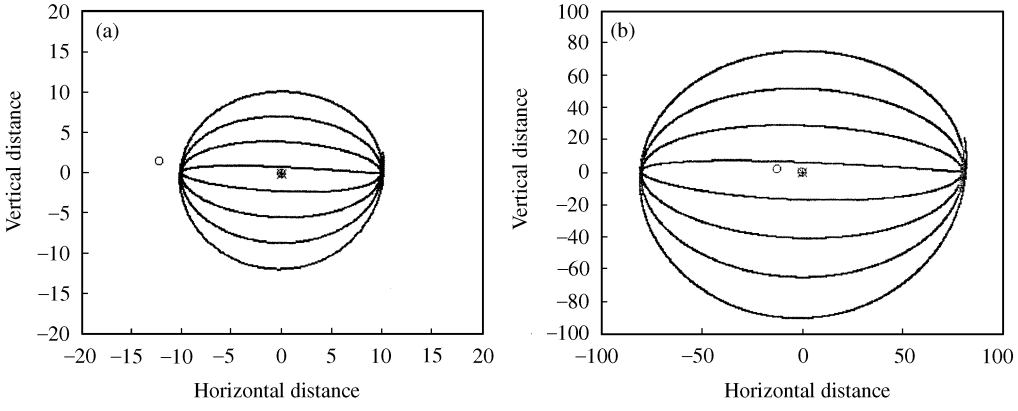

Figure 2. Limit cycle oscillations of a twin conductor bundle: (a) unstable leeward conductor motion slowly diverging to a limit cycle; (b) stable leeward conductor motion slowly converging to a limit cycle (the equilibrium positions of the windward and leeward conductors are shown as an "○" and "★" respectively).

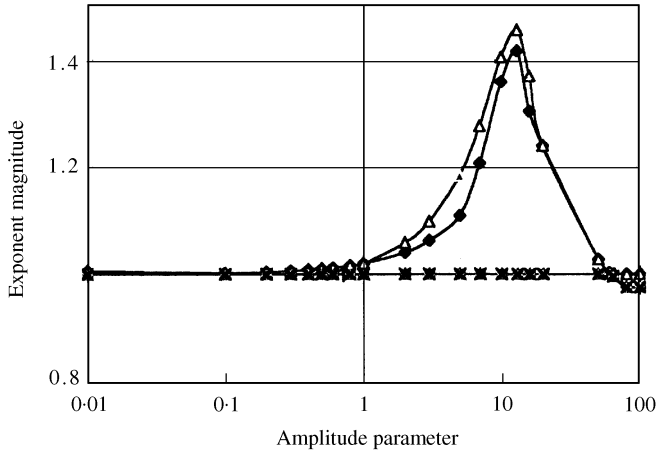

Figure 3. Plot of the maximum and minimum stability exponents for a range of amplitudes of the twin bundle of conductor: Key for matrix exponents: —◆—, monodromy (max); —■—, monodromy (min); —△—, aggregate (max); —×—, aggregate (min).

5. CONCLUSIONS

In this letter, the problem of predicting the stability of non-linear unstable systems characterized by a 1 : 1 internal resonance form of linear dynamics is considered. Two methods of computing the stability exponents are presented and compared by applying to a benchmark application characterized by a slowly evolving limit cycle. The quantitative results obtained match the qualitative results of several previous investigators. Both methods have a distinct advantage over direct numerical integration as the imaginary eigenvalues of the 1 : 1 internal resonance linear dynamics do not actually contribute to the stability exponents. The numerical method incorporates this feature thus ensuring that the computed exponents are reliable and accurate.

The numerical stability exponent prediction techniques may be applied to practical problems well beyond the benchmark problem considered here. Apart from other similar

applications such as the analysis of the stability of periodic orbits (see for example reference [8]), the techniques may be used to alter and control the stability exponents in controlled time periodic systems along the lines suggested by Calico and Weisel [9]. As pointed out by them, the application of Floquet and extended Floquet-type theories to the control problem is quite limited. The methods presented here allows for the fine tuning of the stability exponents after a controller has been designed by certain peliminary approximate methods. A complete discussion of this aspect is beyond the scope of this letter and will be presented elsewhere.

A number of chaotic systems are also characterized by a 1 : 1 internal resonance form of linear dynamics and the techniques presented are currently being evaluated as possible methods for the prediction of the occurrence of chaos. The results of this study will also be presented elsewhere.

Finally, it must be said that while there are a number of other issues associated with the numerical determination of the stability exponents, the objective of this letter was to present a numerical technique not only to predict the complete response of such systems but also to generate an amplitude parameter diagram and reveal features associated with the instabilities. The objective was successfully achieved.

REFERENCES

1. Z. GAJIC and M. LELIC 1996 *Modern Control Systems Engineering*. Engelwood Cliffs, NJ: Prentice-Hall.
2. YU. A. KUZNETSOV 1998 *Elements of Applied Bifurcation Theory*. Applied Maths Sciences, Vol. 112. New York: Springer-Verlag: second edition.
3. W. J. F. GOVAERTS 2000 *Numerical Methods for Bifurcations of Dynamical Equilibria*. Philadelphia, PA: Society for Industrial and Applied Mathematics (SIAM).
4. S. W. SHAW and C. PIERRE 1993 *Journal of Sound and Vibration* **164**, 85–124. Normal modes of non-linear vibratory systems.
5. A. SIMPSON 1971 *Aeronautical Quarterly* **XXII**, 25–41. On the flutter of a smooth circular cylinder in a wake.
6. A. SIMPSON 1971 *Aeronautical Quarterly* **XXIII**, 101–118. Wake induced flutter in critical cylinders: mechanical aspects.
7. G. KERN and A. MAITZ 1998 *International Journal of Non-Linear Mechanics* **33**, 741–751. Normal form transformation and an application to a flutter-type of vibration.
8. W. E. WIESEL and W. SHELTON *Journal of Astronautical Sciences* **31**, 63–76. Modal control of an unstable periodic orbit.
9. R. A. CALICO and W. E. WIESEL 1984 *Journal of Guidance and Control* **7**, 671–676. Control of time-periodic systems.